

Updated Electron Neutrino Appearance Results from MiniBooNE

M. H. Shaevitz^{*†}

Columbia University

E-mail: shaevitz@nevis.columbia.edu

New electron neutrino appearance results are presented for the MiniBooNE experiment at Fermilab with a total data set approximately a factor of 2 larger than previously reported. The new data has a significant excess in the low energy region that is consistent with the previously published MiniBooNE low energy excess results. If interpreted in a standard two-neutrino, $\nu_\mu \rightarrow \nu_e$, oscillation model, the best oscillation fit to the neutrino-mode excess has a χ^2 probability of 15% while the background-only fit has a probability of 0.06% relative to the best oscillation fits. All of the major backgrounds are constrained by in-situ event measurements and so non-oscillation explanations would need to invoke new anomalous background processes or other new physics. The MiniBooNE excess is consistent with the LSND observations as a function of distance/energy (L/E) in the range of overlap. A 3+1 sterile oscillation interpretation for the MiniBooNE/LSND appearance data is in tension with current disappearance results and may require more complicated models and/or new physics.

Neutrino Oscillation Workshop (NOW2018)

9 - 16 September, 2018

Rosa Marina (Ostuni, Brindisi, Italy)

^{*}Speaker.

[†]For the MiniBooNE Collaboration

The MiniBooNE experiment was proposed in the summer of 1997 and has been operating since 2002. The experiment uses the Fermilab Booster neutrino beam where 8 GeV protons are incident on a 71 cm long beryllium target which is inside a toroidal magnetic focusing horn. From 2002-2017, the MiniBooNE experiment has collected a total of 11.27×10^{20} POT in antineutrino mode and 12.84×10^{20} POT in neutrino mode. The neutrino sample has approximately doubled in size since the previous publication [1] in 2013 prompting the publication of updated neutrino results [2]. Charged pion and kaons are focused into a 50 m long decay region which is 91 cm in radius. The main flux of neutrinos is from pion and kaon decay to muon neutrinos but there is also an intrinsic component of electron neutrino flux from kaon and muon decay. In neutrino mode, the ν_μ , $\bar{\nu}_\mu$, ν_e , and $\bar{\nu}_e$ flux contributions at the detector are 93.5%, 5.9%, 0.5%, and 0.1%, respectively, while in antineutrino mode, the flux contributions are 15.7%, 83.7%, 0.2%, and 0.4%, respectively.

The MiniBooNE neutrino detector is located 541 m downstream of the beryllium target. The detector is a spherical tank of inner radius 610 cm and filled with 818 tons of pure mineral oil (CH₂) with a density of 0.86 g/cm³ and an index of refraction of 1.47. Charged particles produce both prompt directional Cherenkov light and longer time constant isotropic scintillation light in a ratio of about 3 to 1 for $\beta \approx 1$ particles. The detector consists of an inner spherical target region of radius 575 cm with 1280 equally-spaced inward-facing 8-inch phototubes (PMT) providing a 10% photocathode coverage; there is also an optically isolated outer veto shield region 35 cm thick with 240 8-inch phototubes. The detector has been designed to detect and measure neutrino events in the energy range from 100 MeV to a few GeV. Event reconstruction [3] and particle identification make use of the hit PMT charge and time information, and the reconstructed neutrino energy, E_V^{QE} , is estimated from the measured energy and angle of the outgoing muon or electron, assuming the kinematics of CCQE scattering.

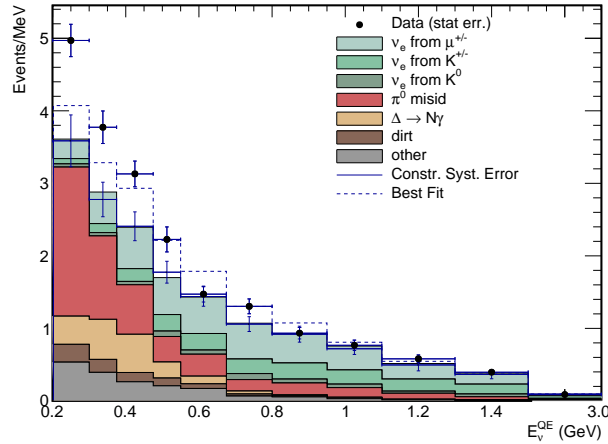


Figure 1: The MiniBooNE neutrino mode E_V^{QE} distributions, corresponding to the total 12.84×10^{20} POT data, for ν_e CCQE data (points with statistical errors) and background (histogram with systematic errors). The dashed curve shows the best fit to the neutrino-mode data assuming two-neutrino oscillations.

The data analysis is optimized to measure ν_e and $\bar{\nu}_e$ induced CCQE events, and the event

reconstruction [3] and selection are identical to the previous analysis [1]. The average selection efficiency is $\sim 20\%$ ($\sim 0.1\%$) for ν_e -induced CCQE events (ν_μ -induced background events) generated over the fiducial volume. The fraction of CCQE events in antineutrino mode that are from wrong-sign neutrino events was determined from the angular distributions of muons created in CCQE interactions and by measuring CC single π^+ events.

An oscillation signal in MiniBooNE would correspond to an excess of candidate electron neutrino events over expectation from backgrounds. The primary uncertainties are associated with the ν fluxes, the ν cross sections, the modeling of the detection and identification efficiencies, and the rates of misidentifications. For MiniBooNE, the main backgrounds to an oscillation ν_e signal are the intrinsic ν_e events along with misidentified neutral current ν_μ produced π^0 , radiative $\Delta \rightarrow N\gamma$, and externally produced γ events. All of the important backgrounds can be directly constrained in both normalization and spectrum from observed non-background events in MiniBooNE; this procedure significantly reduces most of the systematic uncertainties.

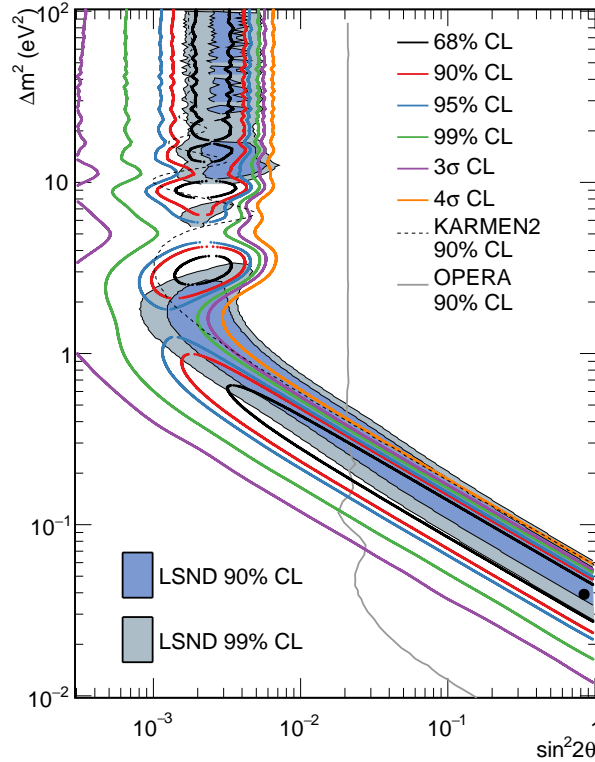


Figure 2: MiniBooNE allowed regions in neutrino mode (12.84×10^{20} POT) for events with $200 < E_\nu^{QE} < 3000$ MeV within a two-neutrino oscillation model. The shaded areas show the 90% and 99% C.L. LSND $\bar{\nu}_\mu \rightarrow \bar{\nu}_e$ allowed regions. The black point shows the MiniBooNE best fit point. Also shown are 90% C.L. limits from the KARMEN [8] and OPERA [9] experiments.

The estimated sizes of the intrinsic ν_e and gamma backgrounds are based on MiniBooNE event measurements and uncertainties from these constraints are included in the analysis. The intrinsic

Table 1: The expected number of unconstrained and constrained background events for the range $200 < E_\nu^{QE} < 1250$ MeV compared to the observed data for neutrino and antineutrino mode.

Process	Neutrino Mode	Antineutrino Mode
Unconstrained Bkgd.	1590.6 ± 176.9	398.2 ± 49.7
Constrained Bkgd.	1577.8 ± 85.2	398.7 ± 28.6
Total Data	1959	478
Excess	381.2 ± 85.2	79.3 ± 28.6

$\nu_e/\bar{\nu}_e$ background from muon decay is directly related to the large sample of observed $\nu_\mu/\bar{\nu}_\mu$ events, as these events constrain the muons that decay in the 50 m decay region. This constraint uses a joint fit of the observed $\nu_\mu/\bar{\nu}_\mu$ and $\nu_e/\bar{\nu}_e$ events, assuming that there are no substantial $\nu_\mu/\bar{\nu}_\mu$ disappearance oscillations. The other intrinsic ν_e background component, from kaon decay, is constrained by fits to kaon production data and SciBooNE measurements [4]. The gamma background from neutral-current (NC) π^0 production and $\Delta \rightarrow N\gamma$ radiative decay are constrained by the associated large two-gamma sample (mainly from Δ production) observed in the MiniBooNE data, where π^0 measurements [5] are used to constrain the π^0 background. Single-gamma backgrounds from external neutrino interactions (“dirt” backgrounds) are estimated using topological and spatial cuts to isolate the events whose vertices are near the edge of the detector and point towards the detector center [6]. Systematic uncertainties in the predicted background and oscillation signal are estimated from variation of the parameters and measurements that go into the predictions. These uncertainties are captured in a covariance matrix in bins of E_ν^{QE} that includes correlations between the predicted ν_e and ν_μ events and that is used in the χ^2 calculation of the oscillation fits.

Fig. 1 shows the E_ν^{QE} distribution for ν_e CCQE data and background in neutrino mode for the total 12.84×10^{20} POT data. Table 1 gives the event numbers for both the neutrino mode and antineutrino mode data and background predictions. Both the unconstrained and ν_μ data constrained background are given. In neutrino mode, the data minus prediction excess is 381.2 ± 85.2 events or a 4.5σ effect. Combining the MiniBooNE neutrino and antineutrino data, there are a total of 2437 events in the $200 < E_\nu^{QE} < 1250$ MeV energy region, compared to a background expectation of $1976.5 \pm 44.5(stat.) \pm 88.5(syst.)$ events. This corresponds to a total ν_e plus $\bar{\nu}_e$ CCQE excess of 460.5 ± 99.0 events with respect to expectation or a 4.7σ excess.

A two-neutrino model is assumed for the MiniBooNE oscillation fits in order to compare with the LSND data [7]. The oscillation parameters are extracted from a combined fit of the observed E_ν^{QE} event distributions for muonlike and electronlike events using the full covariance matrix described previously in the full energy range $200 < E_\nu^{QE} < 3000$ MeV. Using a likelihood-ratio technique [1], the confidence level values for the fitting statistic, $\Delta\chi^2 = \chi^2(point) - \chi^2(best)$, as a function of oscillation parameters, Δm^2 and $\sin^2 2\theta$, is determined from frequentist, fake data studies. With this technique, the best neutrino oscillation fit in neutrino mode occurs at $(\Delta m^2, \sin^2 2\theta) = (0.039 \text{ eV}^2, 0.84)$, as shown in Fig. 2, which also includes the confidence level (C.L.) contours for ν_e appearance oscillations. The χ^2/ndf for the best-fit point in the energy range $200 < E_\nu^{QE} < 1250$ MeV is 9.9/6.7 with a probability of 15.5%. The background-only fit has a χ^2 probability of 0.06% relative to the best oscillation fit and a $\chi^2/ndf = 24.9/8.7$ with a probability of 0.21%.

Fig. 3 compares the L/E_ν^{QE} distributions for the MiniBooNE data excesses in neutrino mode

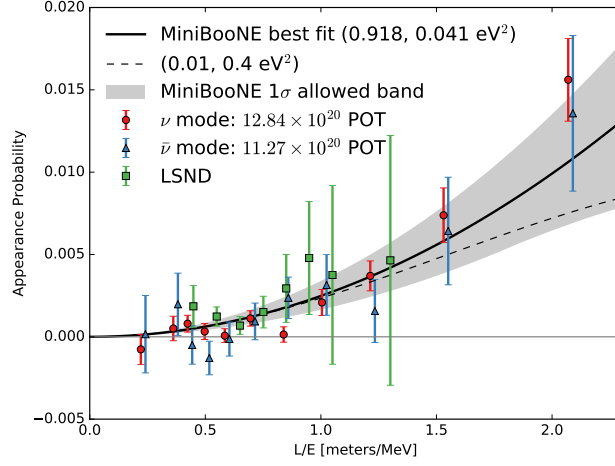


Figure 3: A comparison between the L/E_{ν}^{QE} distributions for the MiniBooNE data excesses in neutrino mode (12.84×10^{20} POT) and antineutrino mode (11.27×10^{20} POT) to the L/E distribution from LSND [7]. The error bars show statistical uncertainties only. The curves show fits to the MiniBooNE data, assuming two-neutrino oscillations, while the shaded area is the MiniBooNE 1σ allowed band. The best-fit curve uses the reconstructed neutrino energy, E_{ν}^{QE} , for the MiniBooNE data. The dashed curve shows the example 1σ fit point.

and antineutrino mode to the L/E distribution from LSND [7]. The error bars show statistical uncertainties only. As shown in the figure, there is agreement among all three data sets. Assuming two-neutrino oscillations, the curves show fits to the MiniBooNE data. Fitting both MiniBooNE and LSND data, by adding LSND L/E data as additional terms, the best fit occurs at $(\Delta m^2, \sin^2 2\theta) = (0.041 \text{ eV}^2, 0.96)$ with a $\chi^2/ndf = 22.4/22.4$, corresponding to a probability of 42.5%. The MiniBooNE excess of events in both oscillation probability and L/E spectrum is, therefore, consistent with the LSND excess of events. The significance of the combined LSND (3.8σ) [7] and MiniBooNE (4.7σ) excesses is 6.0σ , which is obtained by adding the significances in quadrature, as the two experiments have completely different neutrino energies, neutrino fluxes, reconstructions, backgrounds, and systematic uncertainties.

In summary, the MiniBooNE experiment observes a total ν_e CCQE event excess in both neutrino and antineutrino running modes that is consistent with a two-neutrino oscillation interpretation of the LSND experiment. All of the major backgrounds are constrained by in situ event measurements, so non-oscillation explanations would need to invoke new anomalous background or other new physics processes. The MiniBooNE and LSND appearance experiments appear to be incompatible with the disappearance neutrino experiments in a 3+1 sterile neutrino model [10, 11], and other models [12, 13, 14, 15, 16] may provide better fits to the data. The MiniBooNE event excess will soon be studied by the Fermilab short-baseline neutrino (SBN) program [17] using the same beam but with Liquid Argon TPC detectors.

References

- [1] A. A. Aguilar-Arevalo *et al.*, Phys. Rev. Lett. 110, 161801 (2013).
- [2] A. A. Aguilar-Arevalo *et al.*, Phys. Rev. Lett. 121, 221801 (2018).
- [3] R. B. Patterson, E. M. Laird, Y. Liu, P. D. Meyers, I. Stancu, and H. A. Tanaka, Nucl. Instrum. Methods Phys. Res., Sect. A 608, 206 (2009).
- [4] G. Cheng *et al.*, Phys. Rev. D 84, 012009 (2011); C. Mariani, G. Cheng, J. M. Conrad and M. H. Shaevitz, Phys. Rev. D **84**, 114021 (2011).
- [5] A. A. Aguilar-Arevalo *et al.*, Phys. Rev. D 81, 013005 (2010); Phys. Lett. B. 664, 41 (2008).
- [6] A. A. Aguilar-Arevalo *et al.*, Phys. Rev. Lett. 102, 101802 (2009).
- [7] C. Athanassopoulos *et al.*, Phys. Rev. Lett. 75, 2650 (1995); 77, 3082 (1996); 81, 1774 (1998); Phys. Rev. C. **54**, 2685 (1996); **58**, 2489 (1998); A. Aguilar *et al.*, Phys. Rev. D 64, 112007 (2001).
- [8] B. Armbruster *et al.*, Phys. Rev. D 65, 112001 (2002).
- [9] N. Agafonova *et al.*, arXiv:1803.11400.
- [10] S. Gariazzo, C. Giunti, M. Laveder, and Y.F. Li, J. High Energy Phys. 06 135 (2017).
- [11] Mona Dentler, Alvaro Hernandez-Cabezudo, Joachim Kopp, Pedro Machado, Michele Maltoni, Ivan Martinez-Soler, and Thomas Schwetz, J. High Energy Phys. 08 010 (2018).
- [12] J. Asaadi, E. Church, R. Guenette, B. J. P. Jones, and A. M. Szelc, Phys. Rev. D 97, 075021 (2018); G. Karagiorgi, M. H. Shaevitz, and J. M. Conrad, arXiv:1202.1024; Dominik Doring, Heinrich Pas, Philipp Sicking, and Thomas J. Weiler, arXiv:1808.07460.
- [13] Jorge S. Diaz and V. A. Kostelecky, Phys. Rev. D 85, 016013 (2012).
- [14] S. N. Gninenko and D. S. Gorbunov, Phys. Rev. D 81, 075013 (2010); Yang Bai, Ran Lu, Sida Lu, Jordi Salvado, and Ben A. Stefanek, Phys. Rev. D 93, 073004 (2016); Zander Moss, Marjon H. Moulai, Carlos A. Argüelles, and Janet M. Conrad, Phys. Rev. D 97, 055017 (2018); Enrico Baertuzzo, Sudip Jana, Pedro A. N. Machado, and Renata Zukanovich Funchal, arXiv:1807.09877; Peter Ballett, Silvia Pascoli, and Mark Ross-Lonergan, arXiv:1808.02915.
- [15] Jiajun Liao and Danny Marfatia, Phys. Rev. Lett. 117, 071802 (2016).
- [16] Marcela Carena, Ying-Ying Li, Camila S. Machado, Pedro A. N. Machado, Carlos E. M. Wagner, Phys. Rev. D 96, 095014 (2017).
- [17] M. Antonello *et al.*, arXiv:1503.01520; D. Cianci, A. Furmanski, G. Karagiorgi and M. Ross-Lonergan, Phys. Rev. D **96**, no. 5, 055001 (2017) [arXiv:1702.01758 [hep-ph]].